

Spectrometric estimation of leaf pigments in Norway spruce needles using band-depth analysis, partial least-square regression and inversion of a conifer leaf model¹

M. Schlerf^a, C. Atzberger^a, T. Udelhoven^a, T. Jarmer^a, S. Mader^a, W. Werner^b and J. Hill^a

^a Remote Sensing Department, University of Trier, Behringstrasse, D-54290 Trier, Germany, email: schlerf@uni-trier.de

^b Department of Geobotany, University of Trier, Behringstrasse, D-54290 Trier, Germany

ABSTRACT

Empirical and physical approaches to estimate leaf pigments in Norway spruce needles are compared. Foliar samples from 13 stands of Norway spruce, that are heterogeneous in terms of soil nutrient availability were collected (n=78). Foliage was separated by age class and subjected to routine biochemical analysis for chlorophyll *a* and *b*. Needle reflectance of stacked layers was measured using a high spectral resolution spectroradiometer. Three sets of reflectance were used for further analysis: i) 1 nm spectral resolution, ii) degraded to HyMap spectral bands, and iii) HyMap spectral bands with a normally distributed noise component added ($\sigma=0.002$).

From reflectance first-derivative of reflectance, continuum removed reflectance, and normalized band-depths were calculated. Relations between spectra and pigments were developed using stepwise multiple linear regression (SMLR) and partial least square regression (PLSR). The conifer leaf model LIBERTY was inverted using an artificial neural network (ANN). LIBERTY was used in the forward mode to simulate needle stack layer reflectance based on typical leaf parameters. First-derivative of modelled reflectance was used to train the ANN. The trained ANN was then applied to the first-derivative of measured reflectance. For validation purpose the empirical relations and the trained ANN were applied to an independent data set obtained from a different field site. Estimated were compared to measured pigment concentrations.

PLSR performed best on the calibration data set (in terms of r^2 and rmse). On the validation data set, inversion of the LIBERTY model achieved smallest rmse values for the 1st year needles and SMLR for the 3rd year needles.

Keywords: Spectrometry, needle reflectance, leaf pigments, leaf reflectance model, continuum-removal, band-depth normalization, partial least squares regression, artificial neural networks

1 INTRODUCTION

Ecosystem simulation models can potentially be applied to landscapes and regions using remotely sensed information about the biophysical and biochemical state of the canopy [1]. Canopy variables relevant to ecosystem simulation modelling that can be derived from remote sensing are land cover, leaf area index (LAI), and standing biomass [2]. More recently, leaf nitrogen concentration (LNC) has been identified as another major input variable potentially open to remote sensing [3]. LNC or leaf chlorophyll concentration controls the photosynthetic capacity of the foliage and plays an important role in the annual turnover of leaves [4]. Leaves are the most important plant surface interacting with solar energy. Besides canopy structure, the concentrations of the leaf biochemical constituents (pigments, water, protein, cellulose, and lignin) shape the canopy reflectance spectra. Reflectance spectra can be recorded by airborne or spaceborne spectrometers and converted to information on foliar biochemical constituents. This information can then be used to model forest ecosystem processes.

Strong relationships between the concentration of biochemicals and reflectance were found by various researchers for dry and ground leaves using multiple regression techniques [5, 6]. More reliable results were obtained when normalised band depths were used instead of reflectance values [7, 8]. To bridge the gap between established laboratory methods and remote sensing, controlled experiments on fresh whole leaves have been undertaken by various researchers [11-17]. However, the influence of water is strong throughout the near infrared region. Consequently, leaf water can obscure absorption features related to biochemicals, such as protein, lignin, and cellulose in green leaf materials and their estimation from reflectance spectra proved to be rather difficult [9,

¹ Presented at the 3rd EARSeL Workshop on Imaging Spectroscopy, Herrsching, May 13-16 2003

10, 11]. In contrast, the chlorophyll absorption feature is not affected by the influence of water. On the leaf level, good relationships between estimated and measured chlorophyll concentrations were found for various species using empirical [12, 13, 14, 15, 16] and physical approaches [17, 11]. Few studies attempted the estimation of chlorophyll from hyperspectral remote sensing data. For instance, Jago et al. [18] related the red edge inflection point derived from hyperspectral image data to the mean chlorophyll concentration of grassland and winter wheat sites with moderate success. Research on the relation between leaf pigments and laboratory- or field-measured or modelled reflectance is an important step towards their reliable estimation by means of remote sensing. As different methods often lead to dissimilar results, there is a need to compare empirical-statistical and physically-based approaches. Comparing both approaches can also help evaluating the quality of a radiative transfer model.

2 METHODS

2.1 Data collection and data preprocessing

In August 2002, 13 relatively homogenous Norway spruce stands were identified at the Gerolstein test site. Three trees were randomly selected within each stand. Skilled woodsmen climbed the trunks up to the treetop and cut off three branches from the outer part of each crown. Foliage from the sampled branches was removed separately by age class (1st and 3rd year) according to their position on the branch, bagged, labelled and placed in cold boxes in the field. As freezing and thawing are known to change the spectral properties of leaves and needles, the foliage samples were stored in refrigerators at +5°C after the transport to the geosciences laboratory of the University of Trier. In total, 78 samples were obtained (13 stands x 3 trees x 2 age classes). From these samples sub-samples were randomly selected and subjected to standard wet chemical analysis to obtain measures of the concentration of chlorophyll a and b, water, nitrogen, and other chemical elements. Additional sub-samples were randomly selected for reflectance measurements. At another test site (Morbach) samples had been collected in a similar fashion as previously described during March 2000. In total, 30 samples were obtained (5 stands x 3 trees x 2 age classes). Chemical and spectrometric measurements and pre-processing steps were identical for both sets of data.

Chlorophyll concentration was determined by wet chemical laboratory analysis [19]: Approximately 0.5 g of fresh sample was weighted and ground by hand in acetone until no green colour was left in the residual material. After the chlorophyll solution was decanted off the residue, filled up to a volume of 50 ml with acetone, centrifuged for 10 minutes, it was measured in a laboratory spectrophotometer. Chlorophyll a was measured at its absorption maximum of 663 nm and chlorophyll b at 645 nm. Chlorophyll in grams per litre was calculated to milligrams of chlorophyll per gram of dry weight: $Clab [mg g^{-1}] = Clab [g l] \times volume [l] \times 1000 / dry\ sample\ weight [g]$ (Table 1).

Table 1. Summary of data for 3 biochemicals on two dates

Biochemical	Training data, Gerolstein test site, August 2002, n=78, all units: mg g ⁻¹ dry matter				Validation data, Morbach test site, March 2000, n=30, all units: mg g ⁻¹ dry matter			
	Mean	Standard deviation	Minimum	Maximum	Mean	Standard deviation	Minimum	Maximum
Chlorophyll a	2.40	0.45	1.37	3.54	1.46	0.35	0.84	2.60
Chlorophyll b	0.81	0.20	0.42	1.46	0.50	0.15	0.28	0.89
Chlorophyll a+b	3.21	0.64	1.80	4.94	1.96	0.48	1.12	3.43

Reflectance spectra were measured using a Field-Spec-II spectroradiometer under laboratory conditions. The target was illuminated by a 1000 W halogen light source at a zenith angle of 45° and a distance of approximately 60 cm. The optical head of the Field-Spec-II was positioned at nadir (0° viewing angle) at a distance of 10 cm above the target. It was made sure that the instrument's field of view lay well within the target's perimeter. The target consisted of needles arranged in an optical dense layer of about 1 cm thickness over a matt black background. Relative spectral radiances between 350 and 2500 nm were recorded at 1 nm steps in 2151 spectral wavebands. Each sample measurement comprised 50 single measurements of the target and was repeated four times thereby rotating the target to average out any possible directional effects. The reference panel (Spectralon) was measured before and after the target measurements. The absolute spectral reflectance (ρ_{target}) for each waveband was calculated from the radiance counts of measurements of the target (DN_{target}) and the reference ($DN_{reference}$) and the reflectance of the reference ($\rho_{reference}$) as $\rho_{target} = (DN_{target}/DN_{reference}) * \rho_{reference}$. The 5 spectra recorded for each sample

were averaged to produce a single spectrum. The resulting spectra were smoothed using a 31 nm wide moving Savitzky-Golay filter to reduce instrument noise.

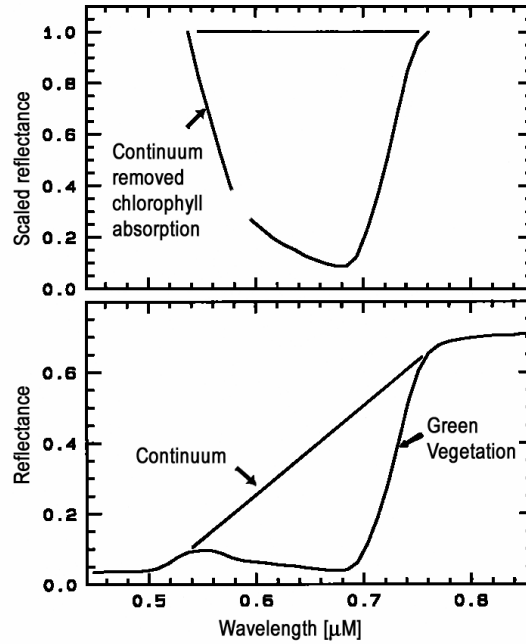


Figure 1: Continuum-removal for chlorophyll absorption in vegetation (from Clark [23]).

To examine the potential of the method at the fresh leaf level to cope with remote sensing measurements of forest canopies, the influence of sensor bandwidth and sensor noise were considered. Three sets of reflectance were used for further analysis: i) 1 nm spectral resolution, ii) degraded to HyMap spectral bands, and iii) HyMap spectral bands with a normally distributed noise component added ($\sigma=0.002$).

Generally, it can be distinguished between empirical-statistical and analytical techniques for the derivation of leaf properties from reflectance data. Empirical models try to find a relation between a vegetation index (VI) or another transformation of reflectance and the leaf parameter. VIs include band ratios, spectral derivatives, spectral shifts, continuum-removal and band depths normalisation. Analytical models, such as radiative transfer models describe the interaction of radiation with leaves based on physical principles. Such a leaf reflectance model relates the spectral information via a complex mathematical function to leaf variables [20]. Once a model is developed, estimates of these variables can be retrieved from reflectance spectra through inversion [21].

2.2 Continuum-removal and band-depth normalisation

Absorptions in a spectrum are composed of the continuum and individual features, where the continuum is the background absorption onto which other absorption features are placed over. The continuum is simply an estimate of the other absorptions present in the spectrum, not including the one of interest [22]. In practice, linear segments can be used to approximate the continuum line. Once this line is established, the continuum removed reflectances (ρ_{CR}) are calculated by dividing the original reflectance values (ρ) by the values of the continuum line (ρ_{CL}) at the corresponding wavelength as $\rho_{CR}=\rho/\rho_{CL}$ [7]. As non-linear multiplicative effects shape reflectance spectra, the continuum should be removed by division and only by subtraction when working with absorption coefficients [23]. The removal of the continuum isolates spectral features and makes them comparable. Continuum removal, for instance, for the chlorophyll feature of green vegetation (Figure 1) may reveal detailed spectral variations of absorption that are not obvious in the original reflectance spectra [23].

Continuum-removed absorption features can be compared by scaling them to the same depth at the band centre. The band depth (ρ_D) at each wavelength in the absorption feature is computed from the continuum-removed reflectance (ρ_{CR}) as $\rho_D=1-\rho_{CR}$. The normalized band depths (ρ_{DN}) are calculated by dividing the band depth of each waveband (ρ_D) by the band-depth at the band center (ρ_{Dc}) as $\rho_{DN}=\rho_D/\rho_{Dc}$ [7]. The main purpose of continuum-removal and band-depth-normalization is the minimization of effects that extraneous factors may have on

reflectance spectra to highlight shape differences of absorption features. Shape differences are then correlated with variations in foliar biochemistry through stepwise multiple linear regression.

2.3 Stepwise multiple linear regression and partial least squares regression

Stepwise multiple linear regression (SMLR) is a technique for choosing variables to include into a regression model. An important underlying assumption is that only some, but not all wavebands do have an important explanatory effect on the leaf chemistry. Forward SMLR starts with no variables in the regression equation; at each step, the most statistically significant variable is added, as specified by the entry criteria (highest F-value or lowest p-value); at the same time the procedure computes the removal statistic for each variable and removes variables if possible (as determined by the removal criteria) Stepping is terminated when neither entry or removal of variables can be performed [24]. Forward SMLR was run on reflectance, first-derivative, continuum-removed and band-depth normalised spectra for wavebands located at the chlorophyll absorption feature between 552 and 749 nm. P-values to enter and remove variables were 0.05 and 0.10, respectively.

Partial least square regression (PLSR) is a spectral decomposition technique that attempts to find latent factors to maximize covariance between the reflectance spectra and chemical concentration. While principal component regression (PCR) performs the decomposition on the spectral data alone, PLSR uses the concentration information during the decomposition process and performs the decomposition on both the spectral and the concentration data simultaneously [25]. One of the main advantages is that the resulting spectral vectors are directly related to the constituents of interest. Due to its superior predictive ability in spectral quantitative analysis [25], PLSR was run on the entire reflectance spectra (400-2500 nm) and the results were considered as the “best estimate possible”. As factor loadings were not considered for interpretation, PLSR served as a sort of black box method. However, comparing results obtained by SMLR (spectral subset) with those of the PLSR (entire spectrum) gave us an indication whether the information necessary to best estimate a particular constituent is entirely contained in the spectral subset or if other spectral absorption features have to be considered.

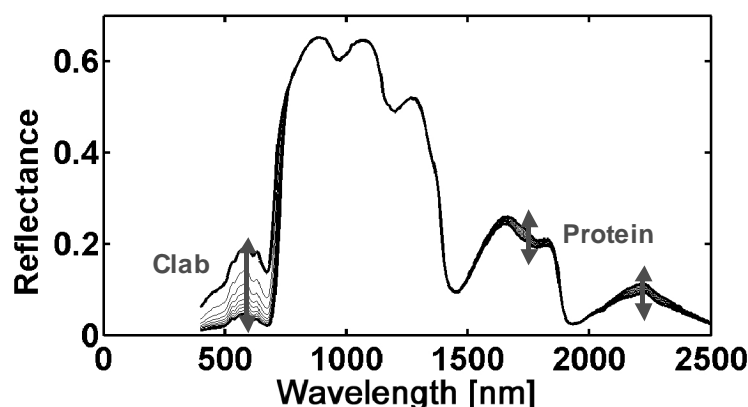


Figure 2: Sensitivity of the LIBERTY-predicted reflectance of a needle stack to variation in chlorophyll a+b content (60-540 g m⁻²) and nitrogen content (0.3-2.1 g m⁻²)

SMLR and PLSR were run separately for 1st year, 3rd year, and both 1st and 3rd year needle samples. In order to test the applicability of the approaches to different data sets and to assess their robustness, regression equations developed from the Gerolstein data set were used to predict the concentrations in the Morbach samples. The accuracy of the estimation on both calibration and validation datasets is reported both in terms of the r^2 between estimated and measured concentrations and the root mean squared error (rmse) of these estimations.

2.4 Inversion of the needle reflectance model LIBERTY

LIBERTY [26] is a general purpose radiative transfer model for simulating the reflectance and transmittance spectra of a conifer needle, or a stacked layer of needles between 400 and 2500 nm. It treats a needle as an aggregation of cells and calculates multiple scattering between cells. Reflectance is modelled as a function of three structural parameters (cell diameter, intercellular air space, leaf thickness) and the combined absorption coefficients of leaf biochemicals (chlorophyll, water, lignin, cellulose, protein). The effects of the variation in chlorophyll and nitrogen content on spectral reflectance are shown in Figure 2. The LIBERTY outputs reveal large effects in the

spectra owing to variation in chlorophyll content while more subtle effects appear due to variations in nitrogen content.

In the direct mode the needle reflectance model computes the spectral reflectance for a certain set of leaf parameters. For the retrieval of leaf parameters from a measured signal it is necessary to invert the model. Due to the complex character of such a model, an analytical solution is not possible and alternative approaches have been developed to successfully invert reflectance models [27]. Traditional inversion of reflectance models employs an optimisation technique to estimate the model parameters by minimising a merit function [21]. An iterative process is necessary to find the optimal estimates of these parameters. The main drawbacks of this method are i) difficulty in achieving globally optimal and stable results and ii) difficulty in retrieving more than 2 parameters simultaneously [28].

Recently, artificial neural nets (ANN) have been employed for reflectance model inversion [28, 29, 30] in order to overcome the above mentioned limitations. To invert a reflectance model using an ANN the following steps have to be carried out [28]: A) Determination of the structure of the ANN, in particular the number of nodes in the input, hidden, and output layer (Figure 3); each spectral band to be used corresponds to a node in the input layer; the number of parameters to be retrieved is the same as the number of nodes in the output layer. B) Simulation of the reflectance spectra from known parameter sets using the reflectance model. C) Presentation of known parameter sets and their corresponding reflectance spectra to the ANN; during the training step an algorithm is used to adjust weights and biases of the ANN in such a way that the rmse between estimated and true parameters is minimized. D) Input of measured reflectance spectra to the previously trained ANN and comparison of parameters estimated by the ANN to measured ones.

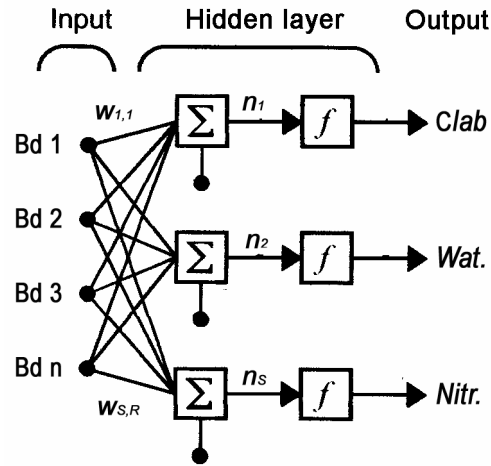


Figure 3: Typical structure of an artificial neural net. After The Mathworks [31]

We used a 2-layer feedforward network for inverting the needle reflectance model. The ANN comprised of three neurons in the hidden layer (tan-sigmoidal transfer function) and 9 neurons in the output layer (linear transfer function). The Levenberg-Marquardt algorithm was employed for training. We randomly generated 6000 parameter sets covering the range of values typical to conifer needles as specified by Dawson et al. [26] and used the LIBERTY model in the stack layer mode to compute the corresponding reflectance spectra. Input reflectances were standardised to a mean of zero and a standard deviation of one. From the standardised reflectances, principal components (PC) were computed. To find proper numbers of required input PC's we experimented with different numbers of PC's defined by the accumulated fraction of explained variance. We finally used the first three PC's explaining 90 percent of the total variance. The number of neurons in the hidden layer was experimentally set to three. All nine LIBERTY parameters were estimated simultaneously.

To compare the chlorophyll contents estimated through LIBERTY (units: mg cm^{-2}) with the chlorophyll concentrations obtained by the chemical analysis (units: mg g^{-1}), contents were converted to concentrations using values of total specific leaf area (SLA_T) as given in the literature. For 1st year needles we used values of $\text{SLA}_{T,1y} = 100.0 \text{ cm}^2 \text{ g}^{-1}$ and for 3rd year needles values of $\text{SLA}_{T,3y} = 88.4 \text{ cm}^2 \text{ g}^{-1}$ that have been obtained by Sellin [32] through measurement of Norway spruce needles collected from tree crowns.

3 RESULTS AND DISCUSSION

3.1 Empirical results

Results of the SMLR and the PLSR on the calibration data set are summarized in Table 2. Between one and three wavebands were selected by SMLR for continuum-removed (CR) and band-depth normalised (DN) spectra. For reflectance and first-derivative spectra (not shown), the number of wavebands selected was generally higher. In the case of CR and DN, most of the selected wavebands could be explained by a relation to either the green peak (540-560 nm), the chlorophyll absorption in the red (640-680 nm), or the red-edge (700-730 nm). For reflectance and 1st derivative of reflectance, less wavebands could be related to these spectral domains. The highest correlation coefficients (*r*) and the lowest calibration errors (*rmse*) were obtained by the PLSR which used between 4 and 12 latent variables to estimate total chlorophyll. For CR and DN, values of *r* were generally lower and values for *rmse* were generally higher using only 1-3 wavebands. PLSR, DN and CR results showed no significant increase in *rmse* when the spectral resolution was reduced to HyMap bands or when noise ($\sigma=0.002$) was added. CR performed particularly well on HyMap spectral bands for 1st year needles; the obtained value of *r* almost reached the value of *r* obtained by the PLSR; however, CR used only two wavebands – one located in the green peak at 549 nm and another placed in the chlorophyll absorption feature at 671 nm, whereas PLSR needed 5 latent variables. On the other hand, for 3rd year needles PLSR (*r* > 0.84) performed much better on HyMap bands compared to CR and DN (*r* < 0.78).

Table 2: *r* and *rmse* between two sets of spectral data and Clab for the wavebands selected by stepwise multiple linear regression; green: 540-560 nm; red: 640-680 nm; red edge: 700-730 nm; spectral coverage: 552-749 nm. PLSR was calculated on the entire spectrum (350-2500 nm)

Data	Sample	SMLR (Continuum removed spectra)			SMLR (Normalized band depth spectra)			PLSR (reflectance spectra)		
		<i>r</i>	<i>rmse</i> cal.	wavebands selected	<i>r</i>	<i>rmse</i> cal.	wavebands selected	<i>r</i>	<i>rmse</i> of calibration	number of latent variables
Original Field-Spec-II (197 bands)	Year 1	.80	.27	713	.87	.22	703, 672	.93	.17	4
	Year 3	.78	.36	748	.85	.31	748, 552, 673	.97	.13	12
	Year 1+3	.87	.33	553, 659, 748	.84	.36	695, 739, 671	.92	.24	5
Resampled to HyMap (15 bands)	Year 1	.91	.19	549, 671	.90	.20	549, 580, 641	.93	.16	5
	Year 3	.78	.36	731, 716	.77	.37	731	.84	.31	4
	Year 1+3	.88	.31	549, 580, 731	.88	.31	549, 580, 702	.92	.25	5
Resampled to HyMap plus noise	Year 1	.80	.27	716	.86	.23	563, 702	.94	.14	5
	Year 3	.77	.37	731, 685	.76	.37	702	.85	.30	4
	Year 1+3	.84	.36	549, 671, 702	.81	.39	702, 549, 731	.93	.24	5

The regression equations derived from the calibration data sets were applied to the spectra from the validation data set in order to estimate biochemical concentrations. There was a considerable decrease in *r* and increase in *rmse* for the chlorophyll estimation on the validation data set compared to the calibration data set (CR, DN and PLSR). For instance, *rmse* increased from 0.21 to 1.44 mg g⁻¹ for the estimation of total chlorophyll from DN spectra of 1st year needles (Figure 4). This increase in *rmse* was more pronounced for 1st than for 3rd year needles. Whereas values of *rmse* were generally higher for 3rd year than for 1st year needles in the case of the calibration data set, values of *rmse* were lower for 3rd year needles compared to 1st year needles on the validation data (CR, DN). A probable explanation for the poor predictive performance of all empirical approaches is the fact that the optical properties of 1st year needles vary considerably with seasonal changes. The predictive equations developed on the needles collected during August could not manage with the reflectance spectra measured on the samples collected during March. The highest validation *rmse*'s were produced by the PLSR for both 1st and 3rd year needles (not shown) and thus seemed to be the less robust of all approaches.

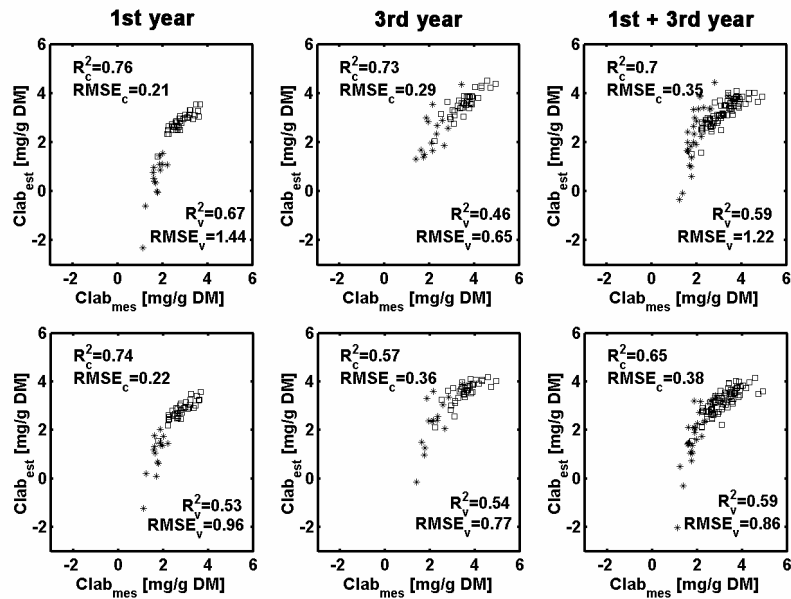


Figure 4: Estimated against measured chlorophyll concentrations using normalized band depth spectra for calibration and validation data sets. Top: 1nm spectra, bottom: resampled to HyMap wavebands + noise. Squares: calibration data set, stars: validation data set.

3.2 Results of the LIBERTY inversion

Mean LIBERTY-predicted and measured (Gerolstein data set) 1st derivative of reflectance agreed well for most wavebands located in the mIR domain, but considerable differences were apparent, particularly in the green, red and certain wavebands in the nIR portion of the electromagnetic spectrum (Figure 5). Obviously, LIBERTY did not properly model the shape of the green peak and the centre of the chlorophyll absorption feature in the red. In the nIR plateau, modelled spectra rather resembled measured spectra of 1st year needles; conversely, 3rd year needle reflectances were dramatically overestimated by the model. As the needle age is not an input parameter to the model, differences in needle age are expressed through needle structural parameters.

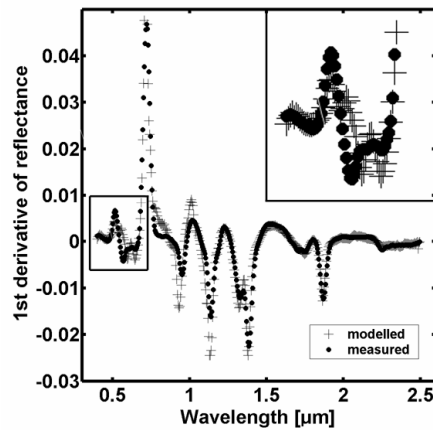


Figure 5: Mean LIBERTY-predicted and measured 1st derivative of reflectance for a needle stack.

The strength of the relationship between estimated and measured chlorophyll concentration is illustrated in Figure 6. Both, the Gerolstein and the Morbach data set, were considered as validation data, as no information inherent to this data, but modelled reflectance spectra had been used to train the neural network. There was a slight difference in the coefficient of determination between estimated and measured chlorophyll concentration for the two data sets; on 1st year needles, the r^2 of the Gerolstein data was greater compared to the Morbach data while the contrary was true in case of the 3rd year needles. Major differences occurred in the rmse as can be seen by the

deviation of the data points from the 1:1-line. Whereas the rmse was relatively small for the 1st year and acceptable for the 3rd year Gerolstein data, it was considerably larger for both age classes of the Morbach data. The needle reflectance model could predict chlorophyll concentrations of needles sampled during August rather accurately but dramatically overestimated the chlorophyll concentrations of the needles sampled during March. Obviously, the needle reflectance model was not able to deal with the optical properties of the spring foliage. Another possible explanation could be that an inappropriate value for specific leaf area had been used.

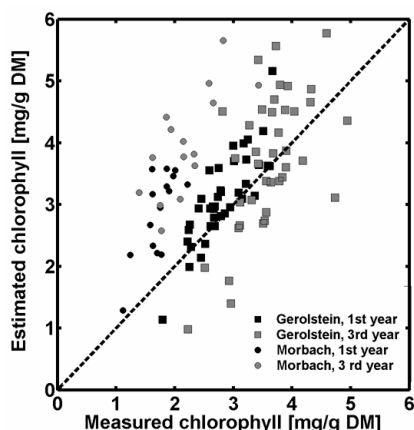


Figure 6: The relationship between measured chlorophyll concentration and chlorophyll concentration estimated through the inversion of a needle reflectance model for two validation data sets (Gerolstein, August, n=78; Morbach, March, n=30).

3.3 Comparison of empirical and physically-based results

1st year needles: In the case of the Gerolstein data, the results obtained by the LIBERTY-inversion were slightly poorer (in terms of the rmse) compared to the results of the empirical approaches. For the Morbach data the physically-based approach yielded a smaller rmse value than the empirical approaches.

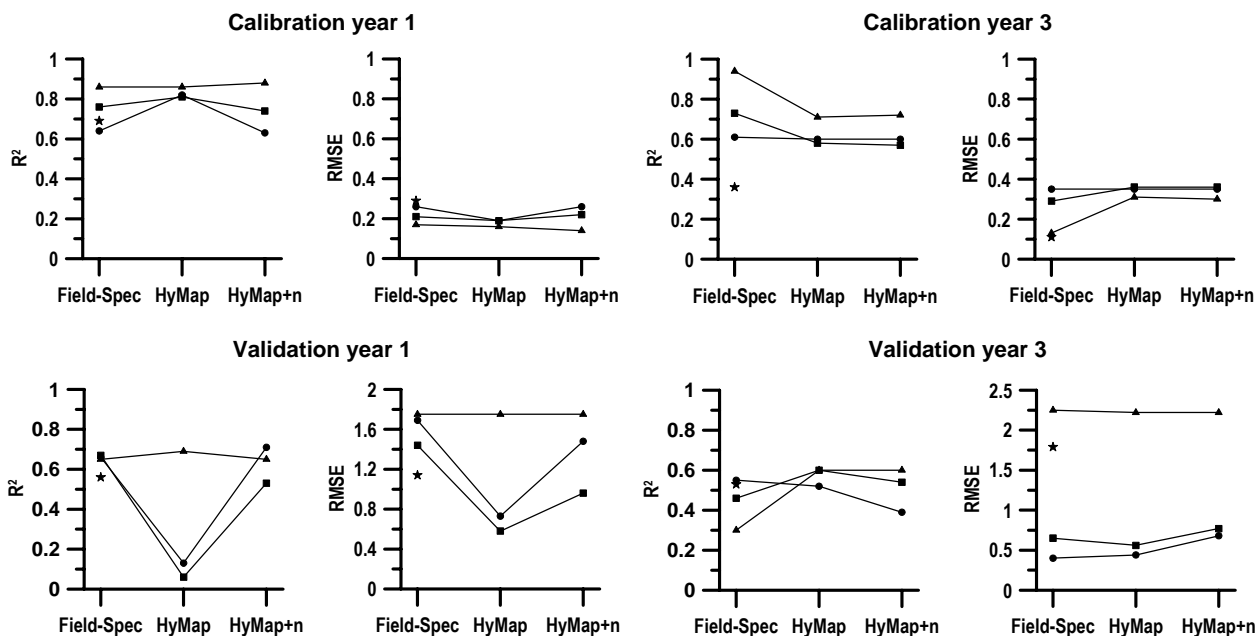


Figure 7: Performance of different methods in estimating total chlorophyll for 1st and 3rd year Norway spruce needles. Datasets: Gerolstein (calibration), Morbach (validation). Spectral resolution of the data: Field-Spec (1 nm spectral resolution), HyMap (Field-Spec spectra degraded to HyMap spectral bands), HyMap+n (HyMap spectral bands with noise added; $\sigma=0.002$). Methods: Stepwise multiple linear regression (SMLR) on continuum-removed spectra (circle), Stepwise MSR on band-depth normalized spectra (square), PLSR on reflectance spectra (triangle), LIBERTY-inversion on first-derivative spectra (star). For the moment, results of the LIBERTY-inversion on spectrally degraded and noisy data has not yet been made available.

3rd year needles: In the case of the Gerolstein data, the PLSR achieved the largest r^2 and the smallest rmse values. The LIBERTY inversion also resulted in low rmse values but the r^2 value was considerably smaller. For the Morbach data, the best chlorophyll estimate was performed by the SMLR on continuum-removed or band-depth normalized reflectance spectra.

4 CONCLUSIONS

The following conclusions can be drawn from the study:

- Leaf chlorophyll in Norway spruce needles could be reliably estimated from continuum-removed (CR) or band-depth normalized (DN) laboratory spectra resampled to HyMap spectral resolution using 2-3 wavebands determined by stepwise multiple linear regression (SMLR). Most of the selected wavebands were located in the green, red, and red-edge domain.
- Noise ($\sigma=0.002$) had a minor (CR, DN) or no (PLSR) influence on the strength of the relations.
- Application of the predictive relations to an independent data set generally yielded a considerable increase of the rmse with all empirical methods. SMLR applied to CR and DN spectra still gave reasonable results for 3rd year needles. PLSR results generally showed the largest rmse and thus, the PLSR method seemed to be the less robust of the empirical methods.
- Inversion of a conifer model using an artificial neural net proved to be more robust than the empirical approaches in estimating leaf chlorophyll of 1st year needles. However, the consistency between LIBERTY-predicted and measured reflectances has to be further improved, particularly in the red domain and the nIR plateau.

ACKNOWLEDGEMENTS

Data collection at Gerolstein test site was supported by the research fund of the University of Trier. The woodmen that did an excellent job were financed by the Forschungsanstalt für Waldökologie und Forstwirtschaft Rheinland-Pfalz. Forest stands were carefully selected with the help of Dr. Schwind, Gerolstein. We thank Samuel, Eva, Lena, and Henning for their assistance in the field and the laboratory. Data collection at Morbach test site was organized by the Department of Biogeography, University of Trier and is highly acknowledged.

REFERENCES

- [1] Ustin, S. L.; Wessman, C. A.; Curtiss, B. et al. (1991): Opportunities for using the EOS imaging spectrometers and synthetic aperture radar in ecological models. *Ecology*, 72: 1934-1945.
- [2] Curran, P. J. (1994): Attempts to drive ecosystem simulation models at local to regional scales. In: Foody, G. M. (Ed.): *Environmental remote sensing from regional to global scales*. Chichester (Wiley):149-166.
- [3] Lucas, N. S. & Curran, P. J. (1999): Forest ecosystem simulation modelling - The role of remote sensing. *Progress in Physical Geography*, 23: 391-423.
- [4] Waring, R. H. & Running, S. W. (1999): Remote sensing requirements to drive ecosystem models at the landscape and regional scale. *Integrating hydrology, ecosystem dynamics and biogeochemistry in complex landscapes 2*: 23-37.
- [5] Card, D. H.; Peterson, D. L.; Matson, P. A. et al. (1988): Prediction of leaf chemistry by the use of visible and near infrared reflectance spectroscopy. *Remote Sensing of Environment*, 26: 123-147.
- [6] Elvidge, C. D. (1990): Visible and near infrared reflectance characteristics of dry plant materials. *International Journal of Remote Sensing*, 11: 1775-1795.
- [7] Kokaly, R. F. & Clark, R. N. (1999): Spectroscopic determination of leaf biochemistry using band-depth analysis of absorption features and stepwise multiple linear regression. *Remote Sensing of Environment*, 67: 267-287.
- [8] Curran, P. J.; Dungan, J. L. & Peterson, D. L. (2001): Estimating the foliar biochemical concentration of leaves with reflectance spectrometry - Testing the Kokaly and Clark methodologies. *Remote Sensing of Environment*, 76: 349-359.
- [9] Fourty, T. & Baret, F. (1998): On spectral estimates of fresh leaf biochemistry *International Journal of Remote Sensing*, 7: 1283-1297.
- [10] Grossman, Y. L.; Ustin, S. L.; Jacquemoud, S. et al. (1996): Critique of stepwise multiple linear regression for the extraction of leaf biochemistry information from leaf reflectance data. *Remote Sensing of Environment*, 56: 182-193.

- [11] Jacquemoud, S.; Ustin, S. L. & Verdebout, J. (1996): Estimating leaf biochemistry using the PROSPECT leaf optical properties model. *Remote Sensing of Environment*, 56: 194-202.
- [12] Curran, P. J.; Dungan, J. L.; Macler, B. A. et al. (1992): Reflectance spectroscopy of fresh whole leaves for the estimation of chemical concentration. *Remote Sensing of Environment*, 39: 153-166.
- [13] Penuelas, J.; Gamon, J. A.; Fredeen, A. L. et al. (1994): Reflectance indices associated with physiological changes in nitrogen- and water-limited sunflower leaves. *Remote Sensing of Environment*, 48: 135-146.
- [14] Datt, B. (1998): Remote sensing of chlorophyll a, chlorophyll b, chlorophyll a+b, and total carotenoid content in eucalyptus leaves. *Remote Sensing of Environment*, 66: 111-121.
- [15] Atzberger, C. & Werner, W.: Needle reflectance of healthy and diseased spruce stands (1998): In: Schaepman, M. et al. (Eds.): 1st EARSeL workshop on imaging spectroscopy: 271-283.
- [16] Daughtry, C. S.; Walthall, C. L. & Kim, M. S. (2000): Estimating corn leaf chlorophyll concentration from leaf and canopy reflectance. *Remote Sensing of Environment*, 74: 229-239.
- [17] Jacquemoud, S. & Baret, F. (1993): Estimating vegetation biophysical parameters by inversion of a reflectance model on high spectral resolution data. In: Varlet-Grancher et al. (Eds.): Crop structure and light microclimate: Characterisation and application. Meeting held at the Chateau de Saumane, Vaucluse, France (INRA-Editions): 339-350.
- [18] Jago, R. A.; Cutler, M. E. & Curran, P. J. (1999): Estimating canopy chlorophyll concentration from field and airborne spectra. *Remote Sensing of Environment*, 68: 217-224.
- [19] Lichtenthaler, H. K. (1987): Chlorophylls and carotenoids, the pigments of the photosynthetic biomembranes. *Methods in Enzymology*, 148: 350-382.
- [20] Goel, N. S. (1988): Models of vegetation canopy reflectance and their use in estimation of biophysical parameters from reflectance data. *Remote Sensing Reviews*, 4: 1-212.
- [21] Goel, N. S. (1989): Inversion of canopy reflectance models for estimation of biophysical parameters from reflectance data. In: Asrar, G. (Ed.): Theory and applications of optical remote sensing. New York (John Wiley & Sons): 205-251.
- [22] Clark, R. N.; Roush, T. L.: Reflectance spectroscopy (1984): Quantitative analysis techniques for remote sensing applications. *Journal of Geophysical Research*, 89: 6329-6340.
- [23] Clark, R. N. (1999): Spectroscopy of rocks and minerals and principles of spectroscopy. In: Rencz, A. N. (Ed.): Remote sensing for the Earth sciences: Manual of remote sensing, 3rd ed., Vol. 3. New York, Chichester, Weinheim (John Wiley & Sons, Inc.): 3-58.
- [24] StatSoft, Inc. (2002): Electronic Statistics Textbook. Tulsa, OK: StatSoft. WEB: <http://www.statsoft.com/textbook/stathome.html>.
- [25] Duckworth, J. (1998): Spectroscopic quantitative analysis. In: Workman, J.; Springsteen, A. W. (Eds.): Applied spectroscopy. A compact reference for practitioners. San Diego, New York, London (Academic Press): 93-164.
- [26] Dawson, T. P.; Curran, P. J. & Plummer, S. E. (1998): LIBERTY - Modelling the effects of leaf biochemical concentration on reflectance spectra. *Remote Sensing of Environment*, 65: 50-60.
- [27] Atzberger, C. (2003): Möglichkeiten und Grenzen der fernerkundlichen Bestimmung biophysikalischer Vegetationsparameter mittels physikalisch basierter Reflexionsmodelle. *Photogrammetrie-Fernerkundung-Geoinformation*, 1: 51-61.
- [28] Gong, P.; Wang, D. X. & Liang, S. (1999): Inverting a canopy reflectance model using a neural network. *International Journal of Remote Sensing*, 20: 111-122.
- [29] Udelhoven, T.; Atzberger, C. & Hill, J. (2000): Retrieving structural and biochemical forest characteristics using artificial neural networks and physically based reflectance models. In: Buchroithner (Ed.): A decade of trans-european remote sensing cooperation. Proceedings of the 20th EARSeL Symposium Dresden, Germany, 14.-16. June 2000: 205-211.
- [30] Kimes, D.; Gastellu-Etchegorry, J. & Estève, P. (2002): Recovery of forest canopy characteristics through inversion of a complex 3D model. *Remote Sensing of Environment*, 79: 320-328.
- [31] The Mathworks (2000): Neural Network Toolbox User's Guide. The MathWorks, Inc. <http://www.mathworks.com/products/neuralnet/>.
- [32] Sellin, A. (2000): Estimating the needle area from geometric measurements: application of different calculation methods to Norway spruce. *Trees*, 14: 215-222.